Hindawi Publishing Corporation
Advances in Condensed Matter Physics
Volume 2012, Article ID 323165, 12 pages
doi:10.1155/2012/323165

Review Article

Broadband/Wideband Magnetoelectric Response

Chee-Sung Park and Shashank Priya

Center for Energy Harvesting Materials and Systems (CEHMS), Department of Materials Science and Engineering, Virginia Polytechnic Institute and State University, Blacksburg, VA 24061, USA

Correspondence should be addressed to Shashank Priya, spriya@vt.edu

Received 19 September 2011; Accepted 26 December 2011

Academic Editor: Amar Bhalla

A broadband/wideband magnetoelectric (ME) composite offers new opportunities for sensing wide ranges of both DC and AC magnetic fields. The broadband/wideband behavior is characterized by flat ME response over a given AC frequency range and DC magnetic bias. The structure proposed in this study operates in the longitudinal-transversal (L-T) mode. In this paper, we provide information on (i) how to design broadband/wideband ME sensors and (ii) how to control the magnitude of ME response over a desired frequency and DC bias regime. A systematic study was conducted to identify the factors affecting the broadband/wideband behavior by developing experimental models and validating them against the predictions made through finite element modeling. A working prototype of the sensor with flat bands for both DC and AC magnetic field conditions was successfully obtained. These results are quite promising for practical applications such as current probe, low-frequency magnetic field sensing, and ME energy harvester.

1. Introduction

Magnetoelectric (ME) materials have been investigated to find applications in sensors, transducers, actuators, energy harvesters, and servomechanism. Direct ME effect implies induction of electric polarization by applying an external magnetic field. It has been widely investigated in composite structures consisting of magnetostrictive and piezoelectric materials. In these composites, ME coefficient is dependent upon the elastic coupling occurring at the interface between piezoelectric and magnetostrictive phases [1–4]. Functional composites are defined by connectivity of materials such as 2-2 composite which is 2 dimensionally laminated, 3-0 composite which has dispersed particles in 3-dimensional matrix, and 3-1 composite which has 1-dmensional rods embedded in 3-dimensional matrix structures. Magnetostrictive-piezoelectric laminate composites with 2-2 connectivity have shown much higher ME coefficients than that of single-phase materials or particulate composites [4–8].

Experimental and analytical results on ME laminates have shown relatively large ME output voltage, but the peak in ME coefficient occurring at the optimum DC bias is generally sharp. This limits their ability to be utilized for AC magnetic field sensing when the optimized DC condition becomes slightly moved off by external noises. Moreover, high ME coefficient generally occurs near the electromechanical resonance (EMR) frequency. This narrow bandwidth also poses problem for stable sensing in a limited frequency range. The common modes utilized for ME laminates are longitudinal transversal (LT) and longitudinal longitudinal (LL). In these two modes, the ME composites exhibit maxima at a specific DC bias magnitude dependent upon the material properties. This maxima position is in the vicinity of ~5 Oe magnetic DC bias for 2-1 composites consisting of Metglas sheets and piezoelectric fibers which is probably the lowest reported value [9]. For sintered composites consisting of PZT and ferrite phases, the maximum occurs at the applied DC bias of ~400 Oe [10].

In order to overcome the problems of limited DC and AC magnetic field ranges associated with laminates, we attempted to design structures with flat ME responses for sensing wide ranges of both DC magnetic field and AC magnetic frequency as illustrated in Figure 1 [11, 12]. Metglas and lead zirconate titanate-lead zinc niobate (PZNT)-based composites were utilized for all the experimentation.

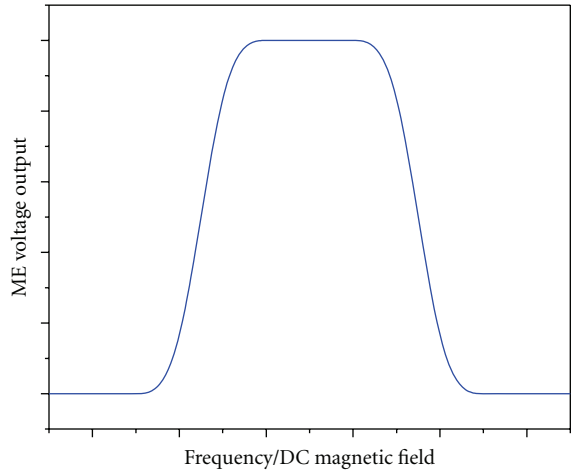

Figure 1: Schematic diagram of an ideal broadband/wideband ME sensor.

2. Broadband Magnetoelectric Composite

Metglas-PZT-based laminate composite structure was selected to understand ME phenomena and to overcome the problem of limited DC magnetic bias operating range. The selection of materials is based upon the fact that high magnetostriction in Metglas occurs at low magnetic DC bias magnitude while the piezoelectric voltage constant (g_{33}) in PZNT is high in the range of 23.41×10^{-3} Vm/N. Dong et al. have shown that the voltage generated through magnetoelectric composite structure is given as [13–15]

$$V = \frac{N d_{33,m} g_{33,p}}{N s_{33}^{E}(1-k_{33}^{2}) + (1-N)s_{33}^{H}} H \cdot t \quad \text{(open circuit voltage)}, \tag{1}$$

where s_{33}^{E} and s_{33}^{H} are the elastic compliances for the piezoelectric and magnetostrictive layers, k_{33} the electromechanical coupling coefficient of the piezoelectric layer, $d_{33,m}$ and $g_{33,p}$ the longitudinal piezomagnetic and piezoelectric voltage coefficients, N is the thickness fraction of magnetostrictive layers, and t is the thickness of piezoelectric layer. This expression is an approximation and requires an additional correction factor to match the magnitude of voltage coefficient measured experimentally. However, it provides an insight into material selection, and based upon this expression it can be seen that piezoelectric voltage constants, elastic compliances (mechanical impedance matching), and piezomagnetic constants ($q_{ij} = \partial\lambda_{ij}/\partial H$) are the key factors controlling the magnitude of ME coefficients.

2.1. Effect of Shape and Laminate Configuration. Piezoelectric square plate and disks with the composition $Pb(Zn_{1/3}Nb_{2/3})_{0.2}(Zr_{0.5}Ti_{0.5})_{0.8}O_3$ [PZNT] were used in this work as schematically depicted in Figure 2(a). The piezoelectric constant of poled PZNT specimens was found to be 500 pC/N, and dielectric constant was found to be 2219 at 1 kHz. On these piezoelectric specimens, 25 μm-thick Metglas (2605SA1, Metglas Inc, USA) sheets of desired dimensions were attached. Twenty layers of Metglas were stacked on one side of square PZNT plate ($15.5 \times 15.5\,mm^2$) to achieve the unimorph structure [Type I]. For the PZNT disk with diameter of 10.2 mm, twenty layers of Metglas were stacked on both sides to form the sandwich structure [Type II]. Figure 2(b) shows the ME responses of both composite structures measured under $H_{ac} = 1$ Oe at 1 kHz. Type I exhibited maximum output voltage of 62 mV/cm.Oe at 215 Oe while Type II showed ME coefficient of 73 mV/cm·Oe at 570 Oe. It is interesting to note that by changing the structure from "unimorph" to "sandwich" and from square shape to disk, the maximum peak position in ME coefficient was shifted by more than 2 times (355 Oe shift). These results bring several interesting questions: (i) what is the effect of stacking configurations on the maximum position of ME coefficient?, (ii) how can the two configurations be combined such that ME coefficient has maximum magnitude over the DC bias range of 215 Oe to 570 Oe?, and (iii) what is the effect of interface area on ME coefficient? These questions will be answered in the next few sections.

2.2. Effect of Number of Metglas Layers. In order to control ME behavior, it is important to understand the role and nature of magnetostrictive layer. The role of number of Metglas layers on ME response was investigated by using the unimorph structure where 2 layers of Metglas with dimension of $7 \times 9\,mm^2$ were incrementally stacked on PZNT plate of $7 \times 15\,mm^2$. Figure 3(a) shows the variation of ME coefficient depending upon the number of Metglas layers and applied DC magnetic field. The composite with 4 layers of Metglas exhibited maximum magnitude of ME coefficient. With further increase in the number of Metglas layers, the ME output steadily decreases. The optimum magnitude of magnetic DC bias was found to increase with increase in the number of Metglas layers. Figure 3(b) summarizes the changes in maximum ME coefficient and optimum DC magnetic field as a function of number of Metglas layers. These results indicate that as the number of Metglas layers increases, higher DC bias is required to reach the maximum ME coefficient. This implies that it is possible to control the ME output value and saturation point by changing the number of Metglas layers.

2.3. Effect of Elastic Coupling on Electrode Structure. In order to gain more insight into elastic coupling process of laminate configuration, a sectioned electrode pattern was designed on PZNT plate of dimension $15.5 \times 15.5\,mm^2$. As schematically shown in Figure 4(a), the electrode pattern on top of the PZNT plate was divided into two parts, a stripe in between the "U" structure. The gap between the two sections was of the order of 1 mm. Ten layers of Metglas was attached on PZNT covering the whole surface area. In the center, on top of the stripe electrode, the number of Metglas layers was increased to thirty layers as shown in Figure 4(a). ME coefficient was first measured separately from the two sections, and then combined response was measured from two sections as shown in Figure 4(b). The ME responses in both scenario were the same regardless

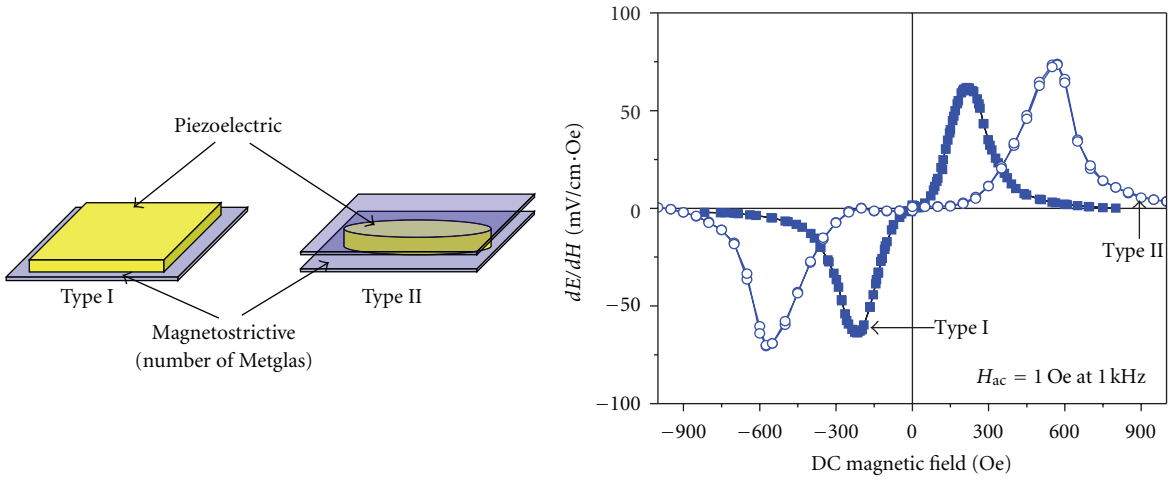

FIGURE 2: (a) Schematic diagram of fabricated samples: type I—15.5 × 15.5 mm^2 PZNT plate with Metglas attached on one side only, and Type II—10.2 mm diameter PZNT disk with Metglas attached on both sides. (b) Magnetoelectric output voltage as a function of DC magnetic field [11].

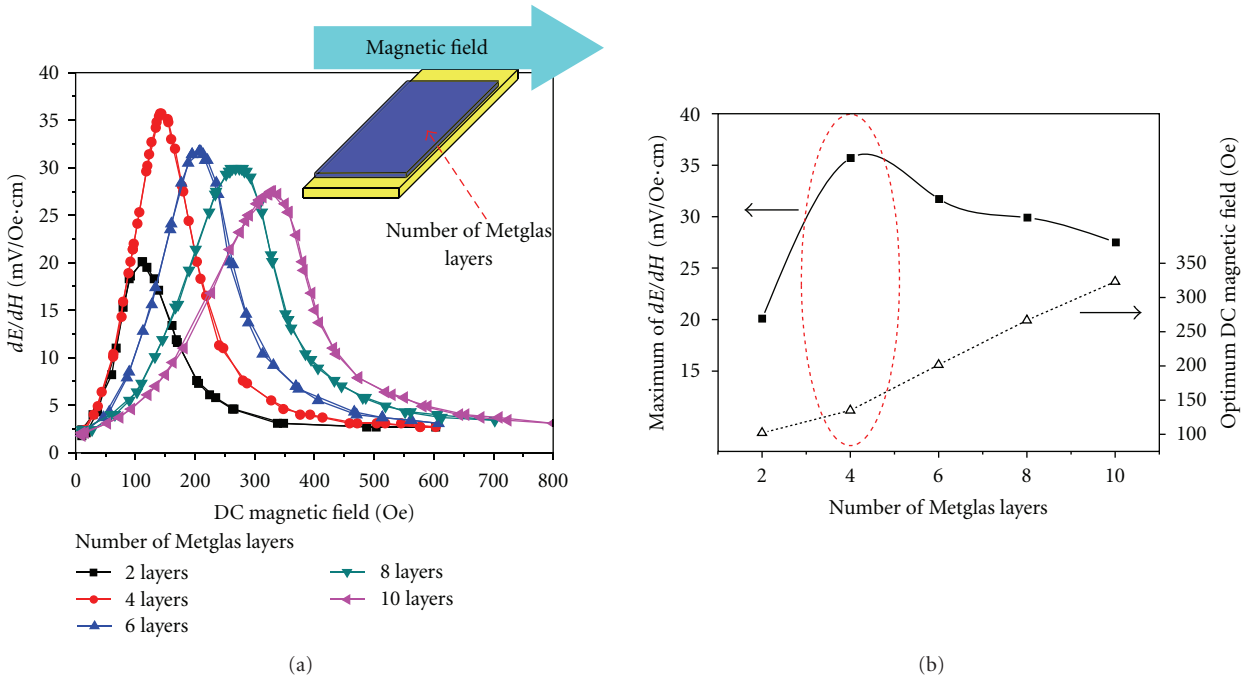

FIGURE 3: (a) ME coefficient as a function of the number of Metglas layers and DC magnetic field. (b) Maximum ME coefficient and optimum DC magnetic field as a function of the number of Metglas layers on PZNT. All measurements were conducted under the constant condition of H_{ac} = 1 Oe at f = 1 kHz [11].

of electrical connections. This phenomenon gives us an important insight. Although locally different ME output behavior was expected from each section because of the difference in number of Metglas layers, the magnitudes of ME coefficient and optimum DC magnetic field were found to be identical from both sections. This indicates that average strain distribution is homogeneous even though locally different strains are generated. Therefore, a larger physical separation will be required to achieve differences between the peak positions of ME coefficient from two separated sections.

2.4. Effect of Composite Dimensions on ME Behaviors. PZNT plates with different planar dimensions (15.5 × 15.5, 12.5 × 12.5, and 8 × 8 mm^2), but the same thickness of 1 mm was used in this experiment. Twenty-layers of Metglas were attached on each plate as shown in Figure 5 (unimorph

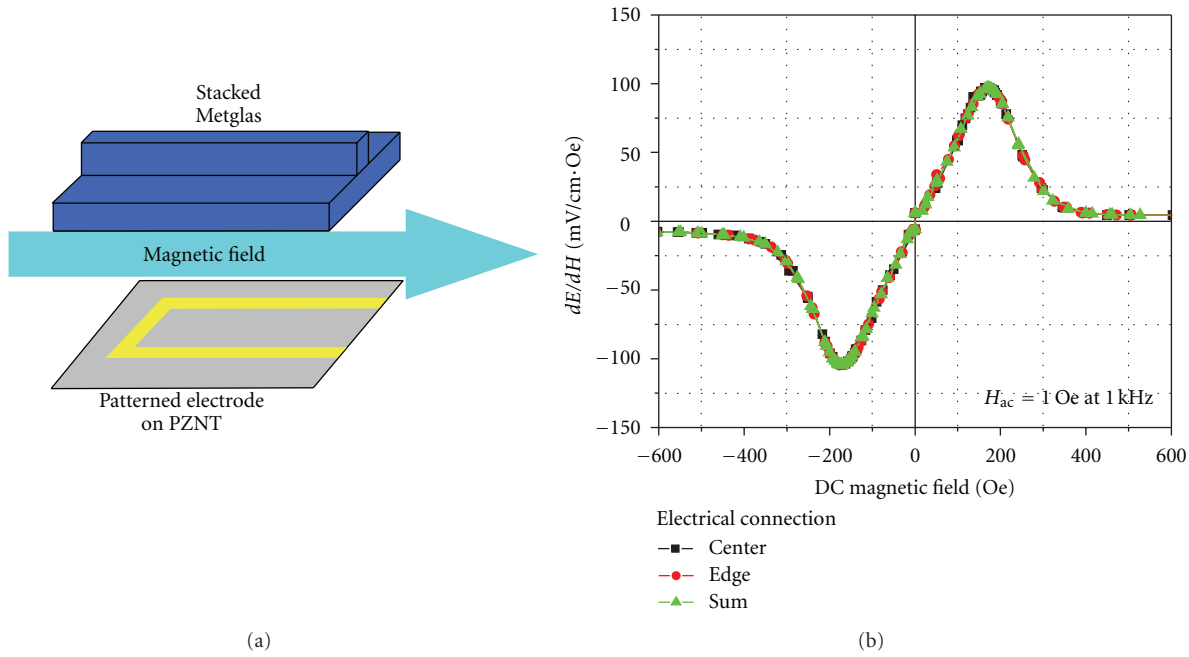

Figure 4: (a) Schematic representation of sample preparation with pyramid-shaped Metglas structure on separately electroded PZNT plate. (b) Magnetoelectric coefficients depending on electrical connections [11].

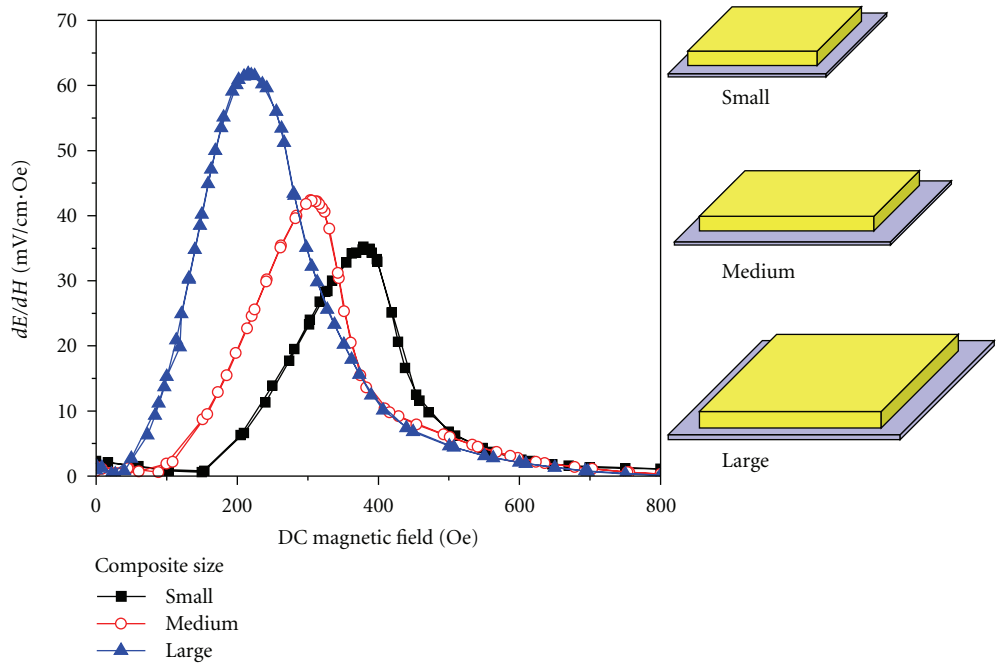

Figure 5: ME coefficient variation as a function of DC magnetic field for various dimensions. 20 layers of Metglas were attached on all PZNT plates. All ME measurements were conducted under H_{ac} = 1 Oe at 1 kHz [11].

configuration). Higher number of Metglas layers was used to avoid variation as a function of number of Metglas layers (saturated response in Figure 3(b)). Thus, the ME coefficient is dependent only upon the planar dimensions of the composite. Figure 5 shows the ME behavior as a function of DC magnetic field for three different samples. As the planar area of composite decreases, the ME voltage coefficient decreases, while optimum DC magnetic field increases. As a result, the ME coefficient and optimum DC magnetic field exhibit inverse behaviors with increasing planar area. In other words, when the planar geometry is larger, the ME coefficient is larger with smaller optimum

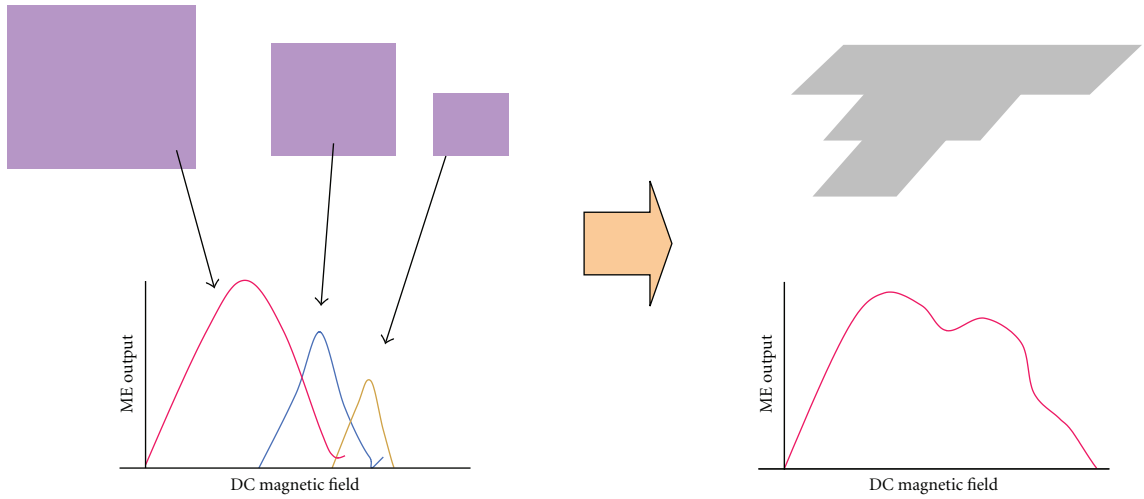

FIGURE 6: Schematic diagram of modified sensor structure. Based on the results of ME dependency on the size (a), dimensionally gradient structure was designed as shown in (b).

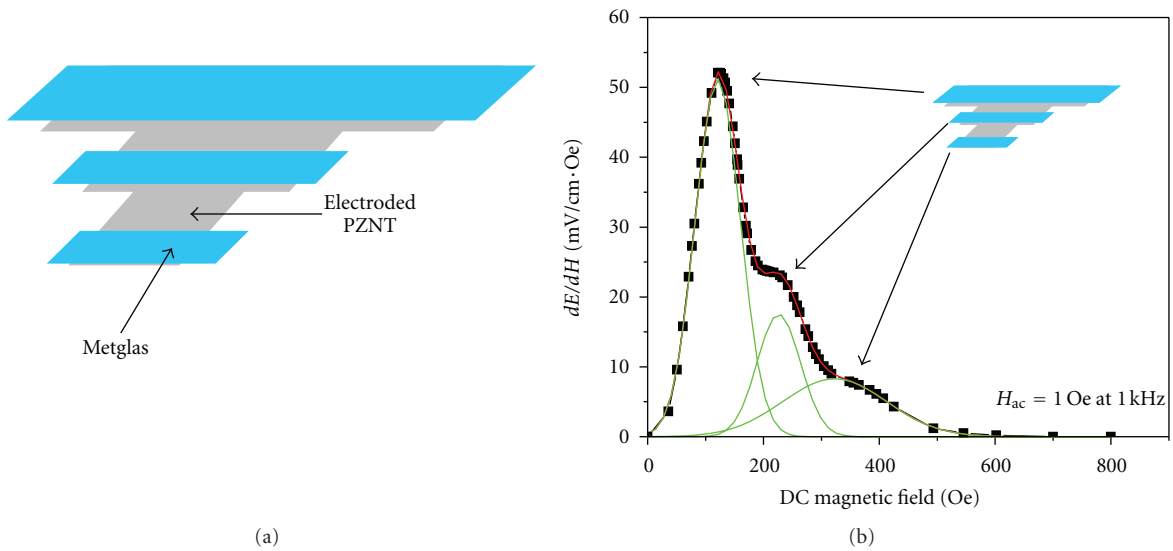

FIGURE 7: (a) Schematic structure of the dimensionally gradient laminate composite. 20 layers of Metglas were attached on each rectangular section, (b) ME coefficient of the dimensionally gradient sample under H_{ac} = 1 Oe at 1 kHz [11].

magnetic DC bias. The results of Figure 5 can be explained on the basis of edge effect called "shear lagging" [16]. As dimensions of ME composites become smaller, the relative surface and edge areas increase leading to shear lagging. This results in the change of magnetization behavior and piezomagnetic coefficient ($q_{ij} = \partial\lambda_{ij}/\partial H$); subsequently, both optimum magnetic bias and ME coefficient are changed with a trade-off relationship between them.

This result is important to realize different peak positions of ME coefficient from different sections. In combination with the result of Figure 3, it is quite interesting to note that optimum number of layers of Metglas on piezoelectric phase with large planar dimensions can provide higher ME coefficient at smaller magnetic DC bias. These results (Figures 3 and 5) lead us to the design rule that maximum peak of the ME coefficient can be shifted by altering the geometry of laminate composites and by designing structure with gradient dimensions as illustrated in Figure 6.

2.5. Effect of Dimensionally Gradient Laminate Composite. In order to achieve the individual response from separated sections of composite, a new geometrical structure was conceived as schematically shown in Figure 6. The composite design was guided by the results of previous sections that indicated (i) different dimensions resulted in different peak positions with respect to magnetic DC bias, and (ii) physical

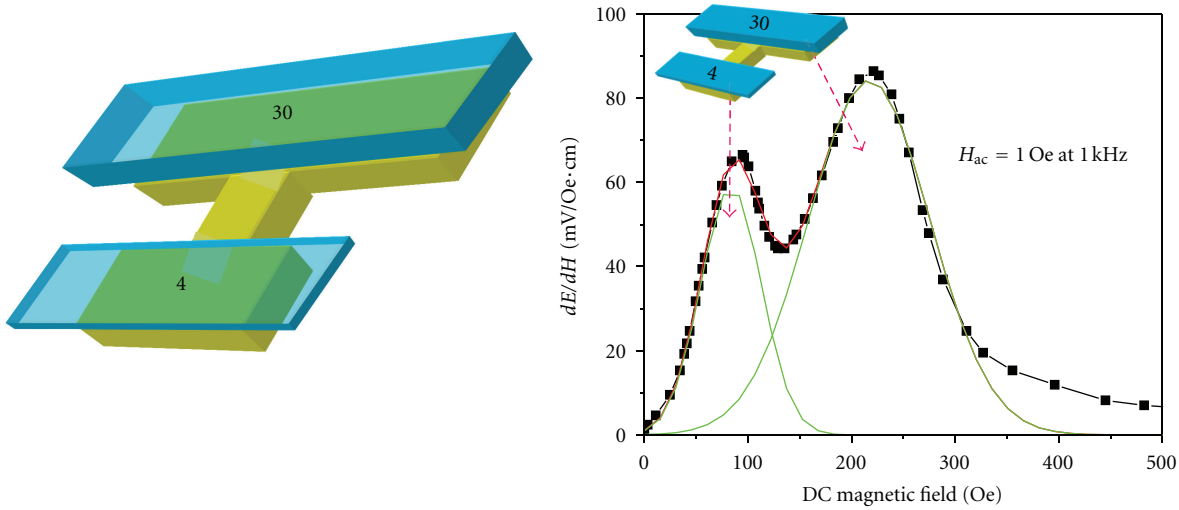

FIGURE 8: (a) Schematic diagram of the asymmetric H-shaped composite structure. (b) Broadband ME behavior of the asymmetric H-shaped laminate [11].

separation between the Metglas layers was necessary to create difference in the peak positions of ME coefficient. We incorporated these two factors by designing a dimensionally gradient composite with the separation of Metglas sections, as shown in Figure 7(a). The dimensions of the PZNT plate in each section were as following: 15.5 × 5, 10.6 × 5.5, and 6.2 × 5 mm^2 (width of about 5 mm was reduced per 5 mm length). The thickness of the plate was 1 mm. On this structure, 20 layers of Metglas with proportional surface area were attached where each Metglas section was separated from each other by 1.5 mm. The stack of twenty-layers of Metglas was intentionally selected so that the observed effect is solely from the variation of the dimension across the composite. Figure 5(b) shows the measured ME response of this composite structure. Interestingly, total ME response of the structure was in combination of the three individual effects as shown by the peak fitting; three-typical components were found in the same specimen. As the planar dimension of composite decreases, the saturation magnetic field increases in providing three separate peaks from three different sections. The larger composite section exhibits higher ME coefficient at smaller magnetic DC bias in agreement with our result in Figure 5 and expectation in Figure 6.

The results of Figures 3–7 lead us to an important conclusion that high magnitude and saturation point of ME coefficient can be controlled by composite structure having separated sections, dimensions of composite, and number of Metglas layers on the piezoelectric planar area.

2.6. Observation of Broadband Behavior. In order to enhance the physical separation, an asymmetric H-shaped PZNT plate was fabricated with the dimensions shown in Figure 8(a) (15.2 × 5.3 and 8.5 × 5 mm^2 areas were connected with the bridge of 4 × 5 mm^2). In this design, the bridge connecting two different dimensions of laminate composites will lead to two separate responses. On this PZNT plate, 4 layers of Metglas were attached on the smaller area, and 30 layers of Metglas were attached on the larger area. It should be noted here that a smaller dimensions lead to smaller ME coefficient, but smaller number of Metglas layers lead to larger ME coefficient. Thus, a compromise between the two opposing effects was calculated to be in the range equivalent to that of the large composite with 30 layers of Metglas. Figure 8(b) shows the measured ME response from this composite structure. The first peak of ME coefficient was found at 94 Oe which was associated with that of 4-layered Metglas structure on smaller piezoelectric surface area. The second peak in ME coefficient was found at 220 Oe resulting from the 30-layered Metglas structure on the larger piezoelectric area. There is a slight drop in the magnitude of ME coefficient between the two peaks, which reflects a mismatch in tailoring the dimensions of two sections. By further adjusting the dimensions, it is possible to bring the two peaks closer to each other and achieve almost a square wave response. However, the results of this figure clearly demonstrate the idea in designing the broadband magnetoelectric sensor.

2.7. Frequency Dependence of Broadband ME Sensor. The frequency dependence of the ME coefficient for broadband composite in the range of 40 to 10^5 Hz is shown in Figure 9(a). The measurement was conducted under the AC magnetic field of H_{ac} = 1 Oe and under applied DC magnetic fields of 94 and 220 Oe. The peaks in this figure correspond to electromechanical resonances occurring at 20, 29, 49, and 70 kHz. It is interesting to note that regardless of the applied DC magnetic field in the range of 94–220 Oe, the broadband ME sensor shows similar range of ME output voltage, ~4 V/cm·Oe, at 49 kHz. The maximum

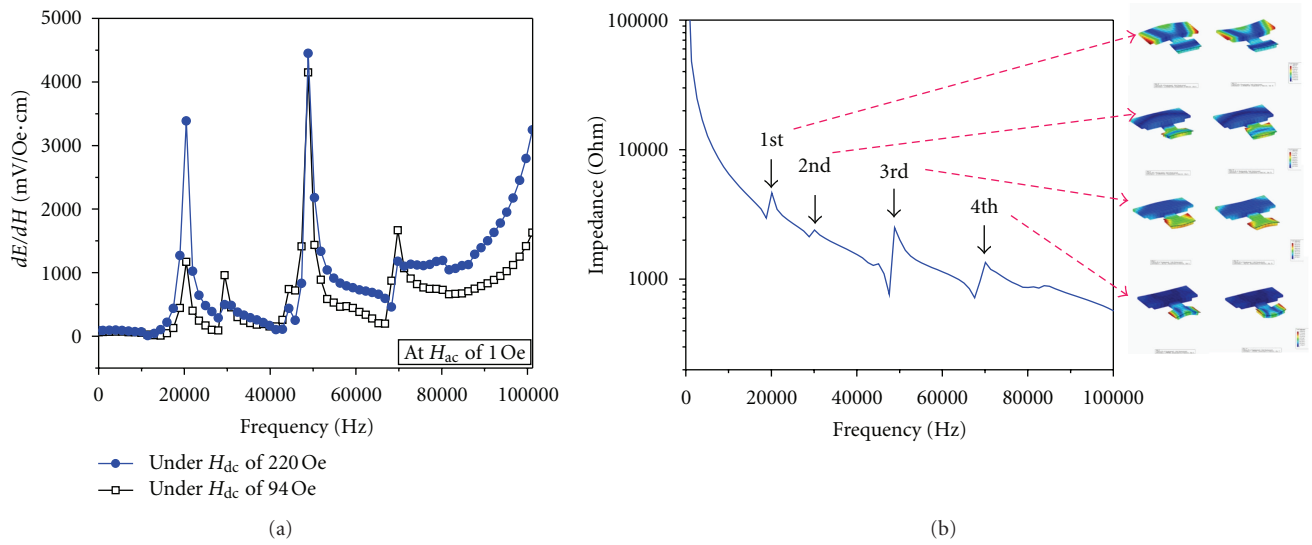

FIGURE 9: (a) Frequency dependence of the ME coefficient for broadband laminate composite. Measurements were conducted under H_{ac} = 1 Oe and H_{dc} = 94 and 220 Oe. (b) Impedance spectrum and FEM analysis of bending resonance modes corresponding to the peak ME responses [11].

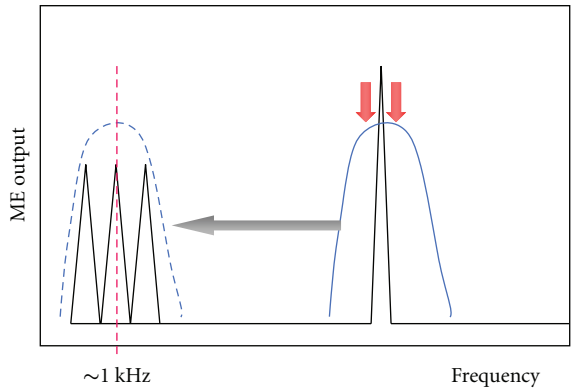

FIGURE 10: Schematic diagram of the goal to achieve wideband ME behavior @ ~1 kHz by generating multiresonances and merging them.

ME output was 4.5 V/cm·Oe under the conditions of H_{ac} = 1 Oe at 49 kHz and H_{DC} = 220 Oe. Figure 9(b) shows the impedance spectrum for H-shaped broadband laminate. The impedance spectrum was found to exhibit resonance peaks at the same position as that observed in ME measurements as a function of frequency. Further, this indicates that all the peaks were correlated to electromechanical resonance modes. An FEM analysis was conducted using ATILA to find the electromechanical resonance modes of the laminate composite. The bending oscillation modes for the four resonances observed in the impedance spectrum are shown in Figure 9(b). The first mode at 20 kHz was found to be from bending of the large rectangular section in the H laminate (Figure 9(b)-1st). The second mode at 29 kHz was found to be from the bending of bridge structure joining the two rectangular sections (Figure 9(b)-2nd). The output voltages from 2nd mode were relatively low which could be associated with the small deformation occurring in the bridge. The third mode at 49 kHz was related to the combined bending response from bridge and small rectangular section of the composite (Figure 9(b)-3rd). This mode generated the highest output voltages as shown in Figure 7. The fourth mode at 70 kHz was found to be related to the bending of small rectangular section of composite (Figure 9(b)-4th). The results indicate that third resonance mode at 49 kHz is combination of second mode occurring at 29 kHz and fourth mode occurring at 70 kHz and leads to larger displacements in the structure resulting in higher ME coefficient. These results further provide the insight in designing a composite structure that could provide large ME coefficient over a wide frequency range.

3. Wideband Magnetoelectric Composite

In previous sections, a near-flat ME response over a magnetic DC bias range of 90–220 Oe at f = 1 kHz was demonstrated by using dimensionally gradient composite structure. Next, we attempt to design composite structure with flat ME behavior as a function of frequency. The electromechanical resonance (EMR) frequency of structure in previous section was still high in the range of 20 kHz, and the ME coefficient exhibited a sharp peak as a function of frequency. As shown in Figure 9(a), the composites generally show enhanced ME coefficient at EMR frequency, but high ME coefficient near EMR is characterized by a sharp peak with very narrow range of magnetic DC bias [3, 14, 17, 18]. In conjunction with the fact that EMR in laminate composites is dependent upon the dimensions, this last observation has limited the application

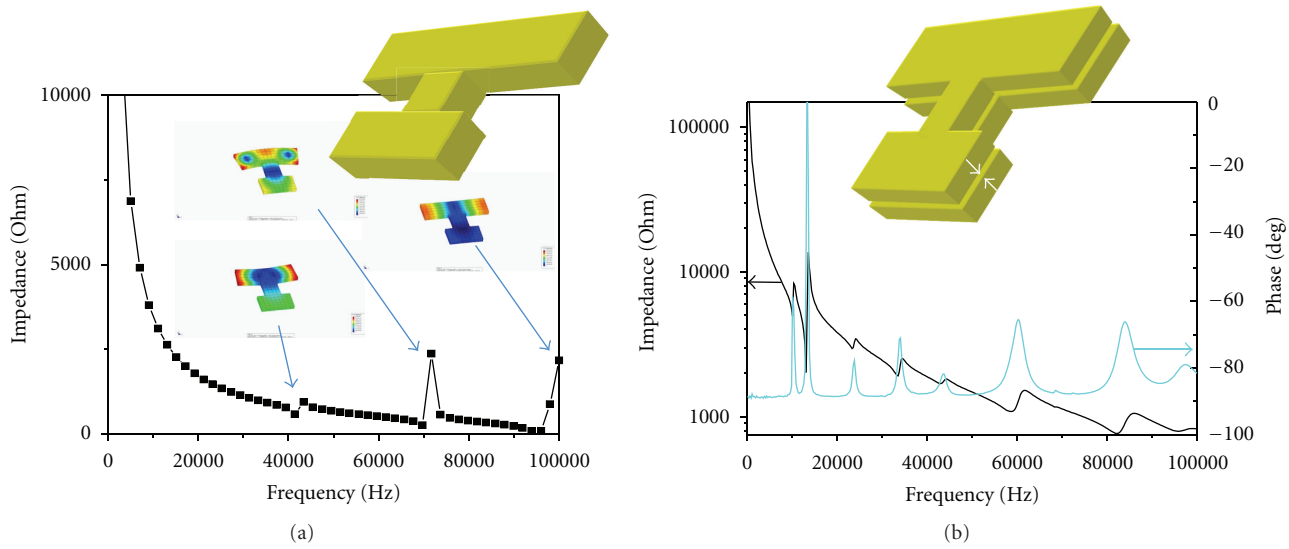

FIGURE 11: Resonance analysis: (a) unimorph and (b) bimorph piezoelectric asymmetric H-shaped structure [12].

of ME composites in magnetic field sensing; that is, large dimensions are required to achieve low EMR frequency.

A study for wideband ME response by combining several Terfenol-D/epoxy-Pb(Zr,Ti)O_3 bilayers through parallel and series electrical connections was conducted by Yu et al. [19]. However, this approach has obvious problems as follows: (i) several laminate composites are required with varying EMR frequency which increases the overall dimensions, (ii) the overall magnitude of ME coefficient at EMR frequency decreases significantly because of mismatch in electrical output, (iii) the magnitude of ME coefficient fluctuates depending upon the gradient in external magnetic field, and (iv) operational frequency is still quite high.

It is well known that, by combining the piezoelectric element having capacitance, C_p, in parallel with shunt having capacitance C_s, the total capacitance of the system changes to $C = C_p + C_s$, which affects the natural resonance frequency (ω) given as [20]

$$\omega = \sqrt{\frac{K_{\text{eff}} + C^{-1}d^2}{m_{\text{eff}}}}, \tag{2}$$

where K_{eff} is equivalent stiffness of the cantilever beam, m_{eff} is the effective mass, and d is the electromechanical coupling. Charnegie has shown that, for a three-layer structure consisting of two piezoelectric beams bonded on to a substrate which is nonpiezoelectric (three layer laminate), the EMR frequency of one piezoelectric layer with capacitance C_p can be shifted by changing the capacitance of other piezoelectric layer C_s through the expression [21]

$$\omega = \sqrt{\frac{3\left(s_{11} - d_{31}^2 A/t\left(C_p + C_s\right)\right)^{-1} I}{L^3 m_{\text{eff}}}}, \tag{3}$$

where A is area, t is the thickness, L is the length, s_{11} is the mechanical compliance of piezoelectric material, d_{31} is the electromechanical coupling coefficient, and I is the moment of inertia. Equation (3) also predicts that by combining several laminates in series and parallel connection the EMR frequency can be modified. This technique has been recently utilized for energy harvesters to modify the operating frequency range [22].

In order to achieve the wideband behavior for the magnetic frequency regime, multiple resonance modes in close vicinity to each other should be the key factor, as schematically illustrated in Figure 10. With reduction in the resonance frequency closer to ~1 kHz, wideband behaviors both in terms of magnetic DC bias and frequency will be described in the next few sections.

3.1. Bimorph-typed Dimensionally Gradient Laminate Composite. Figure 11 shows the difference in resonant frequencies between the asymmetric H-shaped piezoelectric unimorph and bimorph configurations. The resonance spectrum of the asymmetric H-shaped single plate was analyzed using the FEM method (ATILA), as shown in Figure 11(a). The FEM results demonstrate electromechanical resonances occurring at 40, 70, and 94 kHz as shown in Figure 11(a). The first mode at 40 kHz was associated with bending of the larger rectangular section. The second mode at 70 kHz was found to be from bending of two rectangular sections. The third mode at 94 kHz was related to combined lateral response from large rectangular section.

On the other hand, the asymmetric H-shaped piezoelectric bimorph structure was found to generate additional resonant modes and reduce the resonant frequency. Two piezoelectric plates with the thickness of 500 μm were machined to have the asymmetric H shapes (15.5 × 5 and 9.5 × 5 mm^2 areas were connected with the bridge of 4 × 5 mm^2). Next, two piezoelectric plates with opposite poling directions were bonded together as shown in the inset of Figure 11(b). The asymmetric H-shaped bimorph exhibited multiple resonances below 100 kHz as shown in Figure 11(b). The impedance and phase spectrums showed

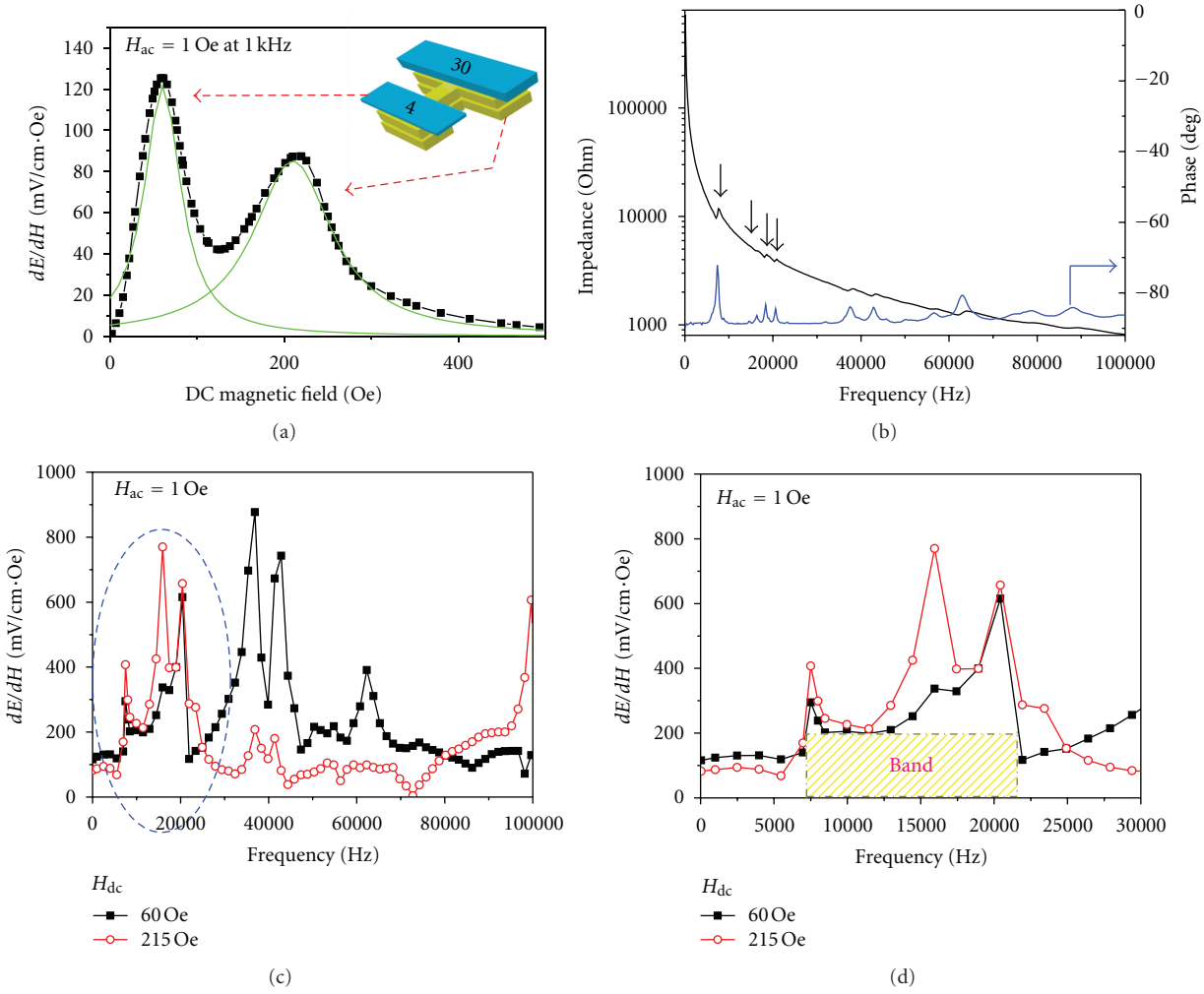

FIGURE 12: (a) ME coefficient as a function of magnetic DC bias at frequency of 1 kHz and applied AC magnetic field of H_{ac} = 1 Oe. Inset: schematic diagram of Metglas attached to the bimorph. Four layers of Metglas of area 15 × 7 mm^2 were attached on smaller rectangular section while thirty layers of Metglas of area 20 × 7 mm^2 were attached on the larger rectangular section, (b) impedance and phase spectrums as a function of frequency, (c) ME coefficient as a function of frequency until 100 kHz, and (d) wideband ME behavior as a function of frequency until 30 kHz [12].

the resonance peaks at 10.09, 13.08, 23.32, 33.31, 43.05, 58.54, and 82.26 kHz. These peaks are resultant of bimorph configuration which indicates coupling between the two piezoelectric plates. The main peak for bimorph was observed at 13.08 kHz. The presence of these additional resonant peaks allows us to merge them in the desired operating range resulting in wide band response.

3.2. Observation of Wideband Behavior. On the asymmetric H-shaped piezoelectric bimorph, four layers of Metglas with area of 15 × 7 mm^2 were attached at the smaller section, and thirty layers of Metglas with area of 20 × 7 mm^2 were attached at the larger section to have configuration similar to that of previous approach (Figure 8(a)). There are two variables here which can be adjusted to achieve averaging of the ME response from two sections of the asymmetric H laminate. First, if the area of two sections is same, then one with smaller number of Metglas layers will show higher ME coefficient. Second, if a number of Metglas layers are same, then one with smaller area will show smaller ME coefficient [11, 12]. Thus, by adjusting the ratio of Metglas layers to area of the piezoelectric rectangular sections, an average response can be obtained from the asymmetric H-shaped structure. Figure 12(a) shows the measured ME response from bimorph composite structure as a function of magnetic DC bias at frequency of 1 kHz with H_{ac} = 1 Oe. The peak at 60 Oe was associated with four-layered Metglas section on the smaller piezoelectric surface area. The second peak of ME coefficient at 215 Oe was associated with thirty-layered Metglas section with the larger piezoelectric area.

Figure 12(b) shows the impedance and phase angle spectrum of this laminate. After Metglas was attached on the PZNT plate, the intensity of resonances became smaller which can be explained by dampening effect and the position

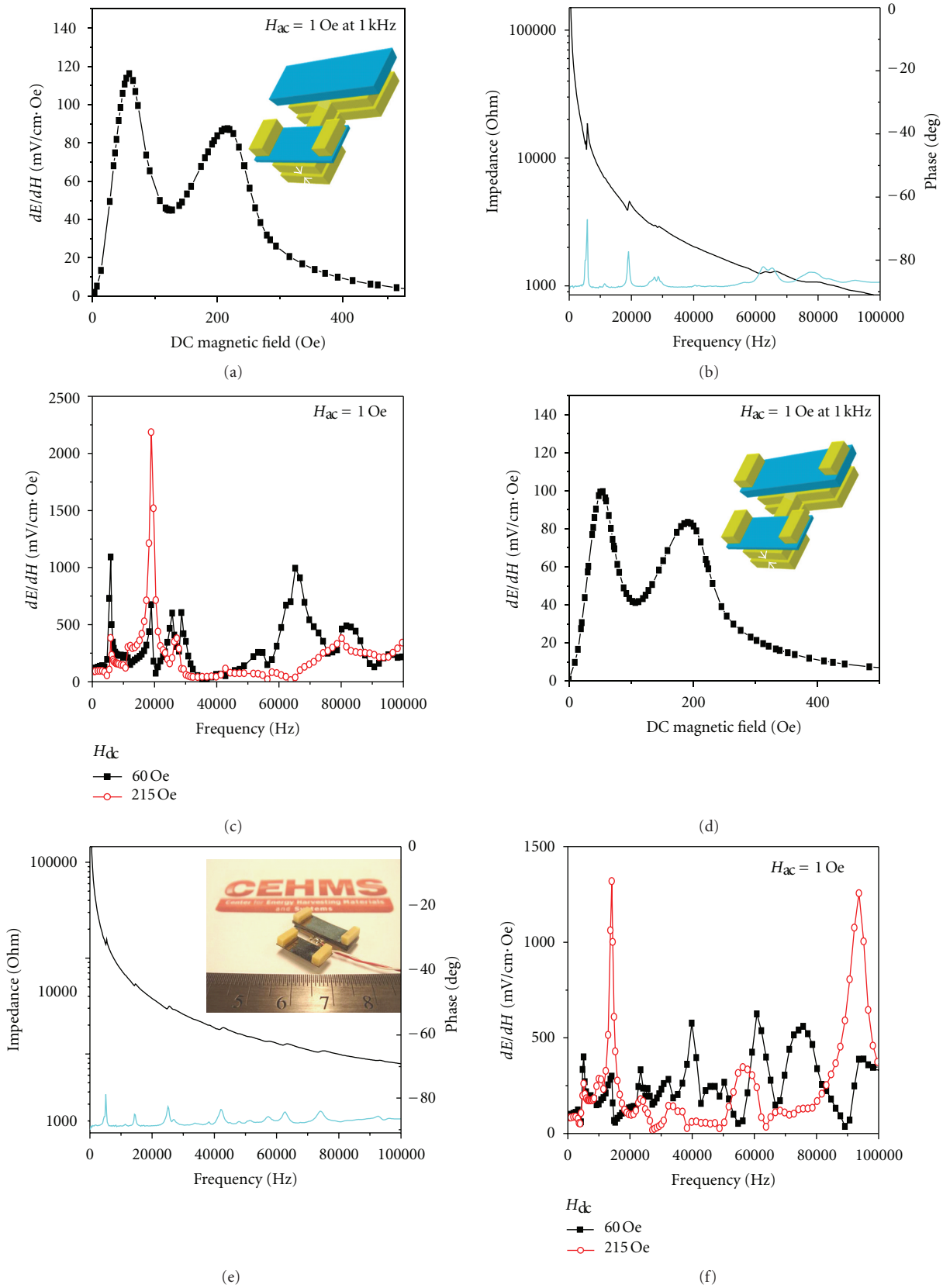

FIGURE 13: (a) ME coefficient of the laminate composite with tip mass on the smaller rectangular area as a function of magnetic DC bias at 1 kHz, (b) impedance and phase spectrums with tip mass on the smaller section as a function of frequency, (c) ME sensitivity with tip mass on the smaller section as a function of frequency, (d) ME coefficient of the laminate with tip mass on both smaller and larger rectangular sections, (e) impedance and phase spectrums with tip mass on both sections, and (f) ME sensitivity as a function of frequency with tip mass on both sections [12].

of peaks shifted towards lower frequencies, in comparison between Figures 11(b) and 12(b). The weight of Metglas on PZNT plates also brought the four peaks initially found at 7.3, 16.3, 18.3, and 20.5 kHz, which originated from the peaks at 10.09, 13.08, 23.32, 33.81, and 43.05 kHz in Figure 11(b), closer to each other. More specifically, the peak at 7.3 kHz in Figure 12(b) was combined with peaks at 10.09 and 13.08 kHz in Figure 11(b).

Consequently, a wideband response was successfully formed in the frequency range of 7–22 kHz, as shown in Figure 12(c) and Figure 12(d). This band comprises of peaks in ME coefficient at 7.5, 15.95, and 20.43 kHz at magnetic DC bias of 60 Oe. Under magnetic DC bias of 215 Oe, the peaks occur at 7.5 and 20.43 kHz. This indicates that the peak at 15.95 kHz was related to magneto-mechanical coupling and not to the electromechanical coupling. The ME sensitivity of the sensor in this band was measured to be higher than 200 mV/cm·Oe which is independent of the magnitude of applied magnetic DC bias.

3.3. Effect of Tip Mass on Wideband Sensor. In order to further reduce the magnitude of resonance frequency, the laminate composite was loaded with a tip mass. According to (2), it can be easily seen that this will result in lowering of the resonance frequency. A tip mass of 0.2 g was placed on both edges of smaller rectangular area, as schematically shown in the inset of Figure 13(a). This figure also shows the effect of tip mass on the ME response as a function of magnetic DC bias at 1 kHz. Figure 13(a) shows no significant change in the ME response as a function of DC magnetic field compared to that in Figure 12(a). However, significant changes were found to occur in ME response as a function of frequency where intensity of peaks in impedance spectrum increased as shown in Figure 13(b), and correspondingly peaks were observed in the ME spectrum shown in Figure 13(c). The magnitude of ME coefficient under 60 Oe magnetic DC bias and frequency of 5.9 kHz was found to be 1092 mV/cm·Oe, and under 215 Oe magnetic DC bias and frequency of 18.9 kHz was found to be 2184 mV/cm·Oe. Comparing with Figure 12(c), this is large increase in ME response. Further, it is interesting to note that the peaks in ME coefficient are at different position under different magnetic DC bias. In terms of wideband width, the tip mass did not result in improvement. For the next step, tip mass of 0.2 g was additionally added on the edges of larger rectangular area, as shown in the inset of Figure 13(d). The first resonance in this case was shifted to ~5 kHz and the numbers of peaks in the impedance spectrum increased as shown in Figure 13(e). As a result, a wideband ME response was obtained in the frequency range of 5–14 kHz with near-flat magnitude of ME coefficient in the range of ~150 mV/cm·Oe, as shown in Figure 13(f). The results in Figures 11–13 clearly show that by using tip mass the resonance behavior can be shifted to lower frequency ranges with wideband response.

4. Summary

Various structural and geometrical parameters were investigated to understand the variation in ME coefficient with applied DC magnetic bias. By controlling laminate dimensions, number of Metglas layers, and gradient geometry, the correlation between the overall deformation and peak position in ME coefficient was found. The broad/wideband ME behavior with near flat ME response was demonstrated by designing a dimensionally gradient bimorph structure and combining with laminate configuration. Using tip masses at the ends of the sensor, wideband frequency response was obtained in lower-frequency range. These results are quite promising for practical applications such as current probe, magnetic field sensing, and ME energy harvester.

Acknowledgment

The authors gratefully acknowledge the financial support from Office of Basic Science, Department of Energy (DE-FG02-08ER46484).

References

[1] N. A. Spaldin and M. Fiebig, "The renaissance of magnetoelectric multiferroics," *Science*, vol. 309, no. 5733, pp. 391–392, 2005.

[2] Y. Lin, N. Cai, J. Zhai, G. Liu, and C. W. Nan, "Giant magnetoelectric effect in multiferroic laminated composites," *Physical Review B*, vol. 72, no. 1, Article ID 012405, 4 pages, 2005.

[3] D. V. Chashin, Y. K. Fetisov, K. E. Kamentsev, and G. Srinivasan, "Resonance magnetoelectric interactions due to bending modes in a nickel-lead zirconate titanate bilayer," *Applied Physics Letters*, vol. 92, no. 10, Article ID 102511, 2008.

[4] J. Ryu, A. V. Carazo, K. Uchino, and H. E. Kim, "Piezoelectric and magnetoelectric properties of lead zirconate titanate/Ni-ferrite particulate composites," *Journal of Electroceramics*, vol. 7, no. 1, pp. 17–24, 2001.

[5] M. Avellaneda and G. Harshe, "Magnetoelectric effect in piezoelectric/magnetostrictive multilayer (2-2) composites," *Journal of Intelligent Material Systems and Structures*, vol. 5, no. 4, pp. 501–513, 1994.

[6] G. Srinivasan, E. T. Rasmussen, B. J. Levin, and R. Hayes, "Magnetoelectric effects in bilayers and multilayers of magnetostrictive and piezoelectric perovskite oxides," *Physical Review B*, vol. 65, no. 13, Article ID 134402, 7 pages, 2002.

[7] J. Ryu, S. Priya, A. Vázquez Carazo, K. Uchino, and H. E. Kim, "Effect of the magnetostrictive layer on magnetoelectric properties in lead zirconate titanate/Terfenol-D laminate composites," *Journal of the American Ceramic Society*, vol. 84, no. 3–12, pp. 2905–2908, 2001.

[8] S. Dong, J. F. Li, and D. Viehland, "Characterization of magnetoelectric laminate composites operated in longitudinal-transverse and transverse-transverse modes," *Journal of Applied Physics*, vol. 95, no. 5, pp. 2625–2630, 2004.

[9] S. Dong, J. Zhai, J. Li, and D. Viehland, "Near-ideal magnetoelectricity in high-permeability magnetostrictive/ piezofiber laminates with a (2-1) connectivity," *Applied Physics Letters*, vol. 89, no. 25, Article ID 252904, 2006.

[10] R. A. Islam and S. Priya, "Large magnetoelectric coefficient in Co-fired Pb $(Zr_{0.52}Ti_{0.48})O_3$-Pb $(Zn_{1/3}Nb_{2/3})O_3$-$Ni_{0.6}Cu_{0.2}Zn_{0.2}Fe_2O_4$ trilayer magnetoelectric composites," *Journal of Materials Science*, vol. 43, no. 6, pp. 2072–2076, 2008.

[11] C. S. Park, C. W. Ahn, J. Ryu et al., "Design and characterization of broadband magnetoelectric sensor," *Journal of Applied Physics*, vol. 105, no. 9, Article ID 094111, 2009.

[12] C. S. Park, C. W. Ahn, S. C. Yang, and S. Priya, "Dimensionally gradient magnetoelectric bimorph structure exhibiting wide frequency and magnetic dc bias operating range," *Journal of Applied Physics*, vol. 106, no. 11, Article ID 114101, 2009.

[13] S. Dong, J. F. Li, and D. Viehland, "Longitudinal and transverse magnetoelectric voltage coefficients of magnetostrictive/piezoelectric laminate composite: theory," *IEEE Transactions on Ultrasonics, Ferroelectrics, and Frequency Control*, vol. 50, no. 10, pp. 1253–1261, 2003.

[14] S. Dong, J. Cheng, J. F. Li, and D. Viehland, "Enhanced magnetoelectric effects in laminate composites of Terfenol-D/Pb(Zr,Ti)O_3 under resonant drive," *Applied Physics Letters*, vol. 83, no. 23, pp. 4812–4814, 2003.

[15] S. Dong, J. F. Li, and D. Viehland, "Magnetoelectric coupling, efficiency, and voltage gain effect in piezoelectric-piezomagnetic laminate composites," *Journal of Materials Science*, vol. 41, no. 1, pp. 97–106, 2006.

[16] C. M. Chang and G. P. Carman, "Modeling shear lag and demagnetization effects in magneto-electric laminate composites," *Physical Review B*, vol. 76, no. 13, Article ID 134116, 2007.

[17] M. I. Bichurin, D. A. Filippov, V. M. Petrov, V. M. Laletsin, N. Paddubnaya, and G. Srinivasan, "Resonance magnetoelectric effects in layered magnetostrictive-piezoelectric composites," *Physical Review B*, vol. 68, no. 13, Article ID 132408, 4 pages, 2003.

[18] Y. X. Liu, J. G. Wan, J. M. Liu, and C. W. Nan, "Numerical modeling of magnetoelectric effect in a composite structure," *Journal of Applied Physics*, vol. 94, no. 8, pp. 5111–5117, 2003.

[19] H. Yu, M. Zeng, Y. Wang, J. G. Wan, and J. M. Liu, "Magnetoelectric resonance-bandwidth broadening of Terfenol-D/epoxy- Pb (Zr,Ti)O_3 bilayers in parallel and series connections," *Applied Physics Letters*, vol. 86, no. 3, Article ID 032508, 3 pages, 2005.

[20] M.G. Muriuki, *An investigation into the design and control of tunable piezoelectric resonators*, Ph.D. dissertation, University of Pittsburgh, 2004.

[21] D. Charnegie, *Frequency tuning concepts for piezoelectric cantilever beams and plates for energy harvesting*, M.S. thesis, University of Pittsburgh, 2005.

[22] H. Xue, Y. Hu, and Q. M. Wang, "Broadband piezoelectric energy harvesting devices using multiple bimorphs with different operating frequencies," *IEEE Transactions on Ultrasonics, Ferroelectrics, and Frequency Control*, vol. 55, no. 9, pp. 2104–2108, 2008.